Available online at www.sciencedirect.com
ScienceDirect
Physica E 37 (2007) 1–5
PHYSICA E
www.elsevier.com/locate/physe

The role of precursor gases on the surface restructuring of catalyst films during carbon nanotube growth

S. Pisana*, M. Cantoro, A. Parvez, S. Hofmann, A.C. Ferrari, J. Robertson

Electrical Engineering Division, Department of Engineering, University of Cambridge, 9 JJ Thompson Ave., Cambridge, CB3 0FA, UK

Received 16 June 2006; accepted 27 June 2006
Available online 7 September 2006

Abstract

Catalyst films undergo considerable surface morphology restructuring prior to carbon nanotube nucleation, deeply influencing the nanostructures obtained. Here we study the influence of different gaseous atmospheres on the structure of thin Fe films. The morphology is influenced by process temperature and substrate interactions and varying the gas type and pressure can control the average catalyst island height.

PACS: 68.35.Ct; 68.37.Ps; 68.55.Jk

Keywords: Carbon nanotubes; Catalysts; Chemical vapour deposition

1. Introduction

Carbon nanotubes (CNTs) are a driving force for current advances in nanotechnology, both on an applied and fundamental level. The ability to control catalyst size and shape are key factors for CNT diameter control [1]. For this, different approaches exist to prepare small isolated catalyst particles, each tailored for different growth methods. In case of surface-bound chemical vapour deposition CNT growth, metallic thin films [2–4] and nanoparticles [5–7] are typically used. However, the high temperatures used during growth, cause the catalyst films to restructure and nanoparticles to merge, thus modifying the final CNT diameter distribution [8]. Indeed, the catalyst's surface morphology before the introduction of the carbon precursor is different than prior to heating it, and its modification can mean the difference between producing carbon fibres or single-wall CNTs (SWNTs) [9]. The nature of the catalyst surface is also crucial during CNT growth, especially at low temperatures, where surface diffusion is the predominant mechanism [9–11].

Here we consider thin catalyst films, and examine, by atomic force microscopy (AFM), their behaviour under different atmospheric pre-growth treatments, in conditions similar to those found prior to CNT growth in both cold-wall and furnace chemical vapour deposition (CVD) chambers.

2. Experimental

High purity Fe thin films were deposited by thermal evaporation on polished boron doped (1 0 0) silicon wafers covered by ~50 nm of thermally grown SiO_2. The oxide layer helps prevent the formation of iron silicides, which otherwise would readily form during thermal annealing through pinholes of the native oxide [12,13]. The evaporation rate was kept below 1 Å/s at a base pressure of $<10^{-6}$ mbar. The film thickness is monitored in situ by a quartz crystal microbalance, and calibrated ex situ by AFM (Veeco Explorer) and spectroscopic ellipsometry (J. A. Woollam Co., M-2000 V).

Thermal annealing of the iron thin films was performed in two different setups, representative of the diverse conditions present just prior to the introduction of the carbon precursor gas and, hence, prior to CNT growth.

*Corresponding author.
E-mail addresses:
sp406@cam.ac.uk (S. Pisana), acf26@cam.ac.uk (A.C. Ferrari).

1386-9477/$ - see front matter © 2006 Elsevier B.V. All rights reserved.
doi:10.1016/j.physe.2006.06.014

Annealing in reduced pressure was carried out in a stainless steel diffusion pumped CVD chamber (base pressure $<10^{-6}$ mbar), on a resistively heated graphite stage. The temperature was ramped at a speed of 50 °C/min in different gases and pressures and kept at the chosen value for 15 min, after which the sample was cooled down in vacuum. The annealing experiments performed at atmospheric pressure were instead carried out in a quartz tube furnace. Here the temperature was ramped up at a speed of 20 °C/min and kept at the chosen value for 1 min.

In both cases, the as grown films were loaded in air and after annealing they were analysed ex situ in ambient conditions, and hence include the effect of oxidation [14]. AFM measurements were performed in tapping mode with etched silicon probes with a tip radius of curvature <10 nm. The AFM tips were frequently changed to exclude the effects of tip wear.

3. Results

Thin metal films nucleate in different modes when deposited, depending on their interaction with the substrate [15]. Strong interactions cause the metal film to "wet" the substrate resulting in layer-by-layer growth mode (Frank-van der Merwe mode [15]) or in islands-on-layer growth (Stranski-Krastanow mode), depending on whether the top layers of the film coalesce into islands to minimize residual strain. On the other hand, weak interactions between metal and substrate result in island nucleation and growth (Volmer-Weber mode), without a surface-wetting layer. For example, Fe grows on SiO_2 in Volmer-Weber mode, since the heat of formation of its oxides (−133.1 to −164.5 kJ/g atom) is higher than that of SiO_2 (−286.7 kJ/g atom), and ultra-thin layers thus consist of isolated islands [16]. As the growing layer thickens the thin film becomes continuous.

If the thin metal film is heated, the mobility of its atoms increases, and the film coarsens and islands coalesce by Ostwald ripening or surface migration, driven by a complex mechanism that minimizes surface energy and/or the free energy of the substrate/metal interface [17–19]. This is strongly dependent on the type of metal, the type of substrate and the annealing environment. The temperature at which metal atoms become mobile and coarsening effects are measurable may be significantly lower than the bulk melting temperature. As a rule of thumb, the Tamman and Huetting temperatures are defined as 0.5 and 0.3 times the melting temperature in Kelvin, and represent the temperatures at which the atoms become mobile in the bulk and at defects, respectively [20]. Therefore, even though Fe melts at 1535 °C, coarsening effects may appear at temperatures as low as 269 °C, although this temperature can be even lower depending on the substrate interactions, size-corrected melting points and the annealing atmosphere [21–23]. For example, Erlandsson et al. [24,25] reported significant restructuring of 0.5 nm thick Pd films (melting and Huetting temperatures of 1554 and 275 °C, respectively) at 200 °C when subject to cyclic exposure to O_2 and H_2.

Fig. 1 shows AFM scans of increasingly thicker Fe films as-deposited and after an anneal at 500 °C in H_2 at 100 mbar. The as-deposited films are relatively smooth but appear discontinuous within the limitations of the AFM and size of tip. The samples annealed in hydrogen are considerably different than the as-deposited samples: Fe agglomerates into discrete islands, which are higher with increasing film thickness. This shows how even a very thin film can agglomerate into islands that are too big to nucleate SWNTs, however, as shown below, the appropriate catalyst film pre-treatment can yield a nanostructured film with islands capable of nucleating SWNTs [9].

Fig. 2 shows the effects of annealing Fe thin films in vacuum or in different atmospheres at a constant pressure of 0.7 mbar and temperature of 500 °C. As expected, thicker films always result in bigger island sizes, however, there is considerable variation in the resulting surface morphology with respect to different annealing atmospheres. Annealing in vacuum yields the highest average island sizes, explaining why generally no CNT growth is obtained when exposed to a carbon precursor gas [26].

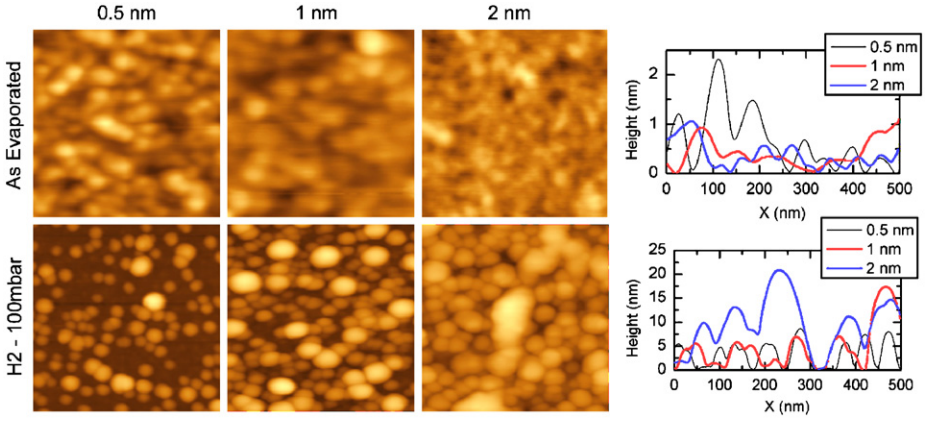

Fig. 1. AFM topography and line profiles of Fe thin films 0.5, 1 and 2 nm thick (left to right), as deposited (top) and annealed at 500 °C in H_2 at 100 mbar (bottom).

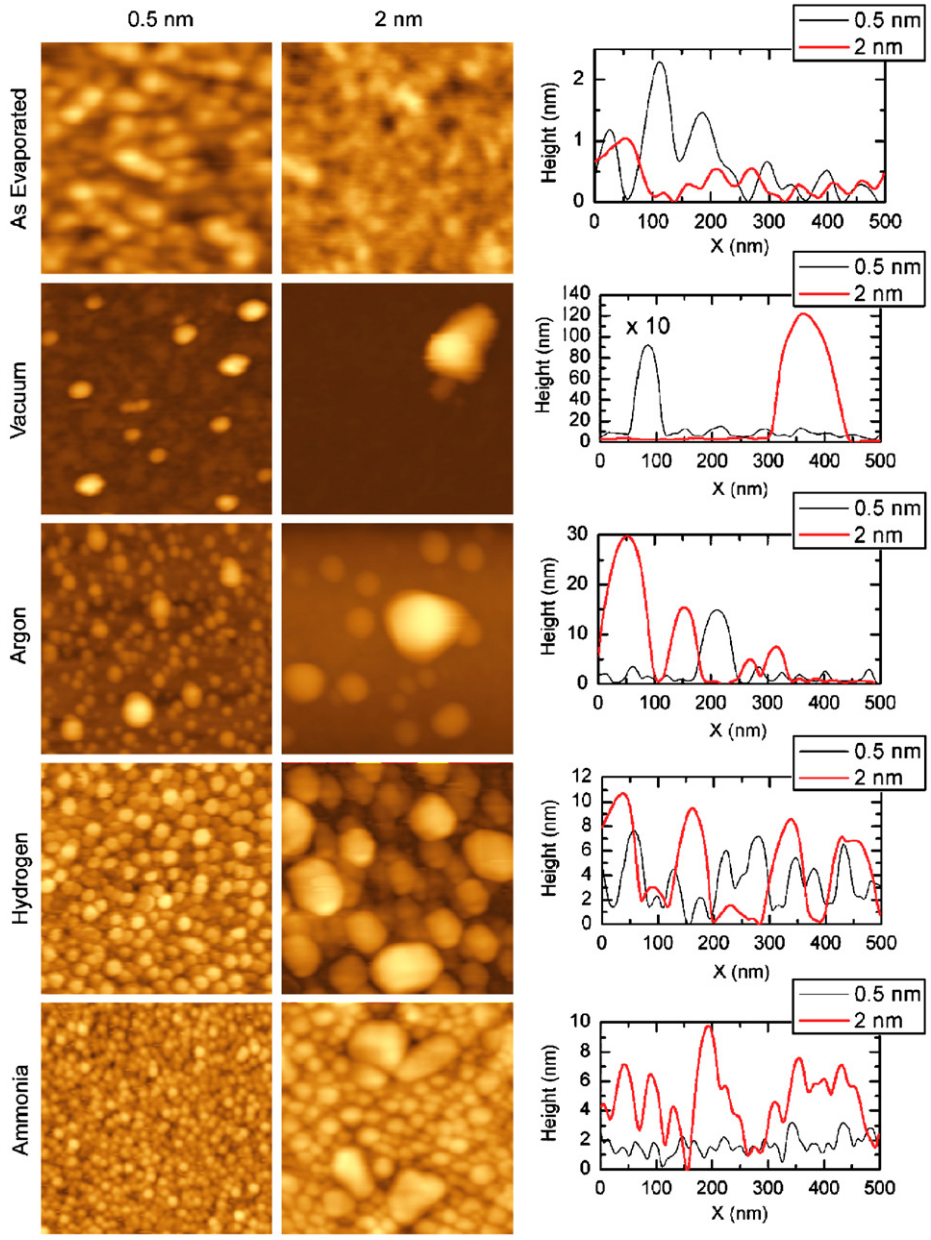

Fig. 2. AFM topography and line profiles of Fe thin films 0.5 and 2 nm thick (left to right), as deposited (top) and annealed at 500° C in vacuum (2nd line, profile for 0.5 nm film multiplied by 10 for clarity), in Ar at 0.7 mbar (3rd line), in H_2 at 0.7 mbar (4th line), and in NH_3 at 0.7 mbar (bottom, data for 0.3 and 2 nm).

The films annealed in Ar, H_2 and NH_3 result in increasingly smaller average island height, with NH_3 being the most effective at restructuring the thin film for SWNT growth. NH_3 or H_2 can reduce oxidized Fe, increasing the surface mobility [27]. Indeed, if the metal strongly interacts with an oxygen-containing substrate or it is oxidized itself, its mobility will be lowered [21]. The reduction of an oxidized metal can also occur following the catalytic decomposition of a hydrogenated carbon precursor [21]. Adsorbed gases also play a role in modifying the mobility of the metal atoms by modifying surface energies and hence affect the catalyst surface reconstruction [28].

Fig. 3 demonstrates how varying the Fe thin film annealing gas pressure can affect the resulting average island height. In general, higher pressures result in lower island heights and narrower island distribution. This can be due to the increase of the interaction between gas and metal, enhancing the effect of the gas. Table 1 contains the island height statistics of all the conditions tested and summarizes the results.

4. Conclusions

The gas type and pressure is found to deeply influence the catalyst morphology. Higher gas pressures are found to

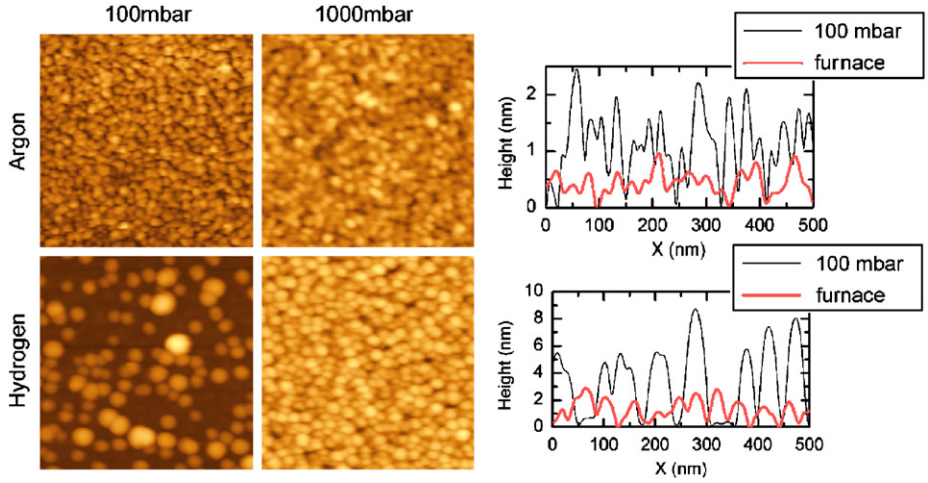

Fig. 3. AFM topography and line profiles of Fe thin films 0.5 thick annealed at 500 °C in Ar (top) and H_2 (bottom), at 100 mbar (left) and in the furnace system (1000 mbar, right).

Table 1
Average Fe island height and standard deviation prior to and after annealing at 500 °C

Gas Type	Pressure (mbar)	0.5 nm film	1 nm film	2 nm film
As Deposited	—	1.1±0.7	0.7±0.2	0.6±0.2
Vacuum	10^{-6}	7.5±3.6	37.4±8.8	94.6±22.0
Ar	0.7	4.2±2.3	5.2±5.4	15.1±17.0
Ar	100	1.1±0.4	1.3±0.5	1.0±0.5
Ar	1000	0.4±0.2	0.4±0.3	0.5±0.3
H_2	0.7	3.8±1.0	4.4±3.4	6.4±3.0
H_2	100	6.8±2.6	8.8±4.9	7.2±2.7
H_2	1000	1.4±0.4	2.7±1.2	7.7±3.1
NH_3	0.7	1.1±0.5*	4.8±2.7	6.5±2.1
Air	1000	0.4±0.2	0.4±0.2	0.6±0.4

Data obtained on $500 \times 500\,nm^2$ scans.
*Data for 0.3 nm film.

be more effective at restructuring the catalyst thin film, yielding catalyst island heights suitable for SWNT growth. Non-reducing environments and interfacial oxygen can help prevent extensive sintering. The detailed investigation of the catalyst's behaviour prior to growth is helpful in explaining its influence on the carbon nanostructures obtained, and it can be extended to nanowire synthesis.

Acknowledgements

The work was supported by the EU project CANAPE. S.H. acknowledges funding from Peterhouse, Cambridge, and A.C.F. from The Royal Society, The Leverhulme Trust and EPSRC grant GR/S97613.

References

[1] H. Dai, Surf. Sci. 500 (2002) 218.
[2] S. Hofmann, M. Cantoro, B. Kleinsorge, C. Casiraghi, A. Parvez, J. Robertson, C. Ducati, J. Appl. Phys. 98 (2005) 034308.
[3] A.J. Hart, A.H. Slocum, L. Royer, Carbon 44 (2006) 348.
[4] Y.Y. Wei, G. Eres, V.I. Merkulov, D.H. Lowndes, Appl. Phys. Lett. 78 (2001) 1394.
[5] Y. Li, W. Kim, Y. Zhang, M. Rolandi, D. Wang, H. Dai, J. Phys. Chem. B 105 (2001) 11424.
[6] A. Javey, H. Dai, J. Am. Chem. Soc. 127 (2005) 11942.
[7] R.M. Kramer, L.A. Sowards, M.J. Pender, M.O. Stone, R.R. Naik, Langmuir 21 (2005) 8466.
[8] O.A. Nerushev, S. Dittmar, R.-E. Morjan, F. Rohmund, E.E.B. Campbell, J. Appl. Phys. 93 (2003) 4185.
[9] M. Cantoro, S. Hofmann, S. Pisana, V. Scardaci, A. Parvez, C. Ducati, A.C. Ferrari, A.M. Blackburn, K.-Y. Wang, J. Robertson, Nano Lett. 6 (2006) 1107.
[10] S. Helveg, C. Lopez-Cartes, J. Sehested, P.L. Hansen, B.S. Clausen, J.R. Rostrup-Nielsen, F. Abild-Pedersen, J.K. Norskov, Nature 427 (2004) 426.
[11] S. Hofmann, G. Csanyi, A.C. Ferrari, M.C. Payne, J. Robertson, Phys. Rev. Lett. 95 (2005) 036101.
[12] M. Liehr, H. Lefakis, F.K. LeGoues, G.W. Rubloff, Phys. Rev. B 33 (1986) 5517.
[13] J.M. Simmons, B.M. Nichols, M.S. Marcus, O.M. Castellini, R.J. Hamers, M.A. Eriksson, Small 2 (2006) 902.
[14] C.M. Wang, D.R. Baer, L.E. Thomas, J.E. Amonette, J. Antony, Y. Qiang, G. Duscher, J. Appl. Phys. 98 (2005) 094308.
[15] J.D. Carey, L.L. Ong, S.R.P. Silva, Nanotechnology 14 (2003) 1223.
[16] R. Pretorius, J.M. Harris, M.-A. Nicolet, Solid-State Electron. 21 (1978) 667.
[17] J.-M. Wen, J.W. Evans, M.C. Bartelt, J.W. Burnett, P.A. Thiel, Phys. Rev. Lett. 76 (1996) 652.

[18] E. Jiran, C.V. Thompson, Thin Solid Films 208 (1992) 23.
[19] P.R. Gadkari, A.P. Warren, R.M. Todi, R.V. Petrova, K.R. Coffey, J. Vac. Sci. Technol. A 23 (2005) 1152.
[20] J.A. Moulijn, A.E. van Diepen, F. Kapteijn, Appl. Catal. A: Gen. 212 (2001) 3.
[21] T. de los Arcos, M.G. Garnier, J.W. Seo, P. Oelhafen, V. Thommen, D. Mathys, J. Phys. Chem. B 108 (2004) 7728.
[22] Y. Qi, T. Cagin, W.L. Johnson, W.A. Goddard III, J. Chem. Phys. 115 (2001) 385.
[23] P.L. Hansen, J.B. Wagner, S. Helveg, J.R. Rostrup-Nielsen, B.S. Clausen, H. Topsoe, Science 295 (2002) 2053.
[24] R. Erlandsson, M. Eriksson, L. Olsson, U. Helmersson, I. Lundstrom, L.-G. Petersson, in: Fifth International Conference on Scanning Tunneling Microscopy/Spectroscopy, Boston, MA, USA, vol. 9, 1991, p. 825.
[25] M. Eriksson, L. Olsson, U. Helmersson, R. Erlandsson, L.-G. Ekedahl, Thin Solid Films 342 (1999) 297.
[26] M. Cantoro, S. Hofmann, S. Pisana, C. Ducati, A. Parvez, A.C. Ferrari, J. Robertson, Diamond Relat. Mater. 15 (2006) 1029.
[27] I. Sushumna, E. Ruckenstein, J. Catal. 94 (1985) 239.
[28] W.F. Egelhoff Jr., D.A. Steigerwald, J. Vac. Sci. Technol. A 7 (1989) 2167.